Chapter 1

Statistical Properties of Images

1.1. Introduction

1.1.1. *Why study statistical properties?*

The analysis of statistical properties of images is dictated by the concern of adapting secondary treatments such as filtering, restoring, coding and shape recognition to the image signal. The basic techniques implemented to suppress a noise or increase a weak signal all rely on hypotheses regarding what is the signal and what is noise, i.e. on signal and noise models. Statistical techniques, taken from signal processing methods, make the assumption that signals are Gaussian or uniformly distributed within an interval for example and white noise, i.e. microscopic correlation signals. From these models, we can deduce, using rigorous sequences, the optimality of a filter or the estimate of its performance, in the average or the worst case. The validity or quality of the coder filter or detector depends practically on the adequacy of the hypotheses that form the base of its calculation and the properties presented by the real-life signal.

Early on, we measured the statistical properties of images and attempted to deduce models that make it possible to explain the images. These statistical models however have very little significance in our daily life because they have less use than structural or syntaxic descriptions that give each image a representation based on natural and geometric language, such as: “a woman with an enigmatic smile, arms crossed on her chest in front of a mountain scape”.

Chapter written by Henri MAÎTRE.

However, in the objective of automatic processing by computer, statistical representation is quite useful as it immediately feeds algorithms that are more or less elaborate and that manipulate pixels, the basic components of the image. The universality of coders such as JPEG or MPEG, which rely greatly on this type of property, is an attestation of the technical interest of these studies.

Our procedure will be as follows: first, we will review the simplest statistical measures, those that are obtained by one-dimensional scanning of the image. We will deduce a model that is used universally. We will show the limits. We will present a few two-dimensional properties that are not covered well by this model. We will suggest improvements to the basic model.

1.1.2. *What images?*

An experimental study must distinguish between two types of very different images:

– incoherent images (this is the case of video images as well as most satellite and medical photos) obtained with incoherent natural light or radiation;

– coherent images, such as those obtained by holography, by radar or ultrasound imaging, in seismic imaging.

The first are obtained by the summation of energy of radiation emitted by various objects associated with a basic pixel.

The second are formed by complex amplitude addition of radiation issued from objects constituting a single pixel. This radiation, according to whether it is in phase or in opposition to phase, will create a clear or dark pixel, these variations depending less on objects that constitute the pixel than on the conditions of propagation, the phase terms depending notably on the geometry of observation. These images, given the often rough surface quality of the objects in the scale of the incidental wave length, are generally marred by a very significant noise called speckle (in radar and astronomy) and granularity (in optics). The statistical properties of coherent images are always very different from those of incoherent images. This chapter addresses incoherent images, which are the most frequent. The properties of coherent images, however, will be repeated when they are well-known.

Our intention is also to determine the properties of the images in general, the images usually encountered. However, even these terms poorly define our objective, as there is no normality in an image. However, they clearly exclude images that are too simple: the “white square on a white background” of painters, the checker board or grid, as well as “pathological” images that represent particular motifs (rosettes,

mosaics, etc.). When required, we will specify what can be normal or abnormal in image processing. Let us keep in mind, however, that normal images form the essential part of video scenes, satellite images, medical images, robotics and microscopic images.

Opera Girls VLSI

Figure 1.1. *Three "random" images*

1.2. Amplitude

1.2.1. *Properties*

We will represent the image by a continuous function, $f(x,y)$, or by a discrete function, $f(i,j)$, of the two space variables x and y, or i and j. We will also frequently use the one-dimensional restriction obtained by line-by-line scanning $f_j(i)$ which we will write as $f(i)$ when there is no ambiguity. We will sometimes limit variables i and j to N and M to return the final dimensions of the images. However, we will therefore choose very large values for N and M. The simple properties in which we are interested to begin with are linked to the amplitude of the image. In most cases, the images are represented in 8 bits, sometimes in 10, 12 for good-quality images or, exceptionally, 16. The first description of interest is the histogram of the amplitude that expresses the frequency of appearance of the various levels.

The images consisting of multitudes of samples (between 100,000 and several million), we often invoke the central limit theorem in order to justify the hypothesis that the image's amplitude will be Gaussian. This is not generally true. The examples in Figure 1.2 present typical histograms of the three images in Figure 1.1. They are unspecified and any other shape would also be possible: the histogram of an image is no more Gaussian than it is uniform.

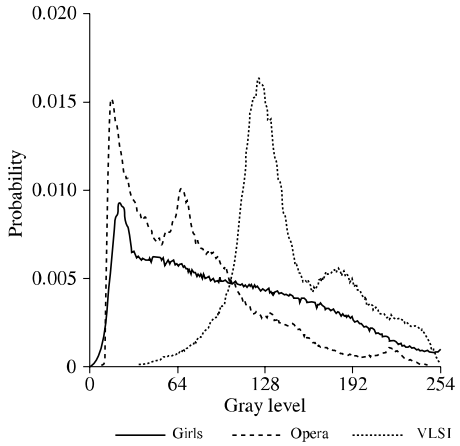

Figure 1.2. *Histograms of the three images of Figure 1.1*

1.2.2. *Sensitivity to modifications of histograms*

We can study in greater detail the dependence of the image's appearance on its histogram. Several interesting studies have been conducted by Estournet [EST 69] who recreated several copies of a single photo on various mediums: photographic paper of different marks, gradations and hardness. The analysis of these documents in Figure 1.3 clearly shows large differences in the histograms, even more noticeable than those that affect the images themselves. Estournet deduced that the image's histogram is not only not significant of this (since obviously much of the images will have very similar histograms taking into account the small dimensions of the histograms), but can also be artificially modified without greatly affecting the exterior aspect of the image and especially without altering the significance of the image.

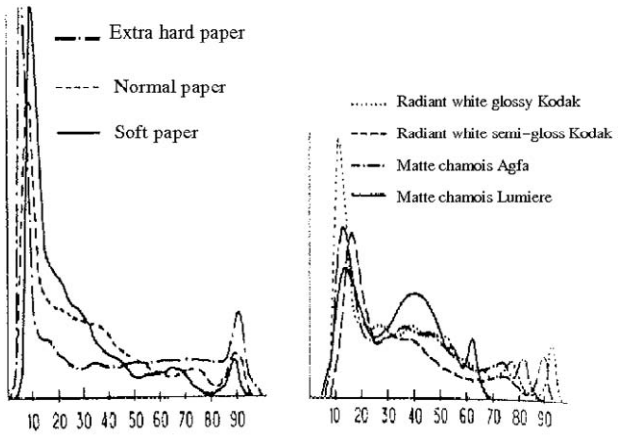

Figure 1.3. *Histograms of the same image obtained for presentations on different types of papers: on the left, paper hardness; on the right, appearance of the paper (according to [EST 69])*

This procedure can be pushed even farther. Could an image have an unspecified histogram? To answer this question, we will use a program that modifies the gray levels in the image by a code conversion that guarantees that the resulting image will have a predetermined histogram. Let us impose a constraint to ensure that the image aspect will remain relatively unchanged: that the relationships of order between gray levels are not lost, i.e. that if n_1 and n_2 are two gray levels verifying that $n_1 < n_2$, then we will transform them into m_1 and m_2 such that $m_1 \leq m_2$. Such a program is easy to conceive. Applied to images, it gives the results in Figure 1.4 where the arrival histograms are a uniform law, a sum of 2 Gaussians and a sine curve respectively. We perceive, of course, differences in the images thus created, but the images remain perfectly recognizable and their interpretation is not affected. This experiment confirms the very superficial role of the histogram whose shape is only distantly linked to the significant elements of the image.

Are these conclusions always valid? Of course not, since very specific images can have very specific histograms: a checker board will be composed of two peaks and black text on white will show two clearly separate modes. If we take a field of very regular waves or a rough-cast wall, it is equally possible that we could obtain Gaussian histograms.

In the case of images obtained with coherent illuminations, we can theoretically carry out the calculation of the probability law of the amplitude reflected by a rough uniform surface (so-called “fully developed speckle” hypothesis [GOO 76]).

We thus show that we obtain, for the probability of a module of complex amplitude, Rayleigh's law:

$$p(f) = \frac{f}{\sigma^2} \exp\left(-\frac{f^2}{2\sigma^2}\right). \qquad [1.1]$$

We verify in Figure 1.5 that the histogram follows this model precisely.

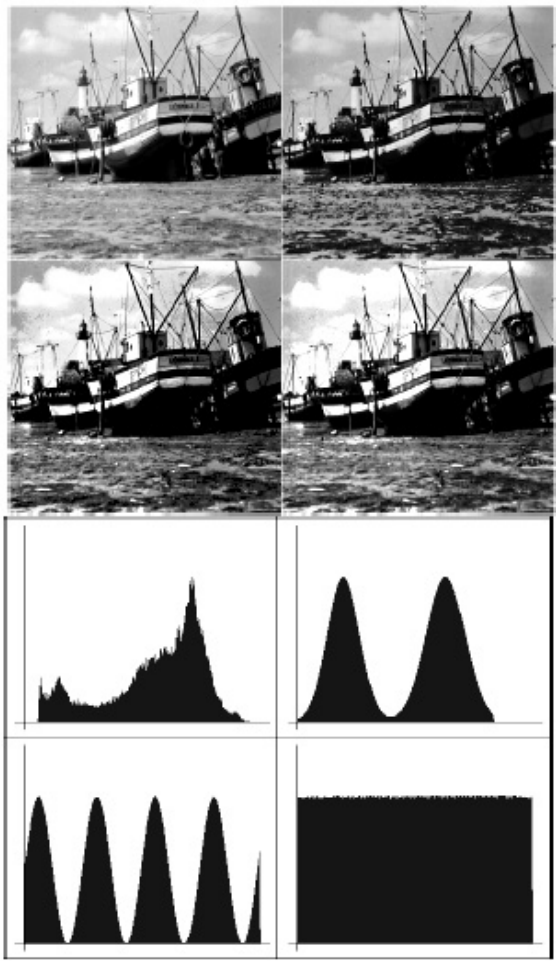

Figure 1.4. *Modification of histogram. At the top left: original picture; at the top right: sum of 2 Gaussians; at the bottom left: sine curve; at the bottom right: uniform distribution*

1.3. Jumps in amplitude

Let us define an amplitude jump as the difference between gray levels of two adjacent pixels along a line: $s_j(i) = s(i) = f_j(i + 1) - f_j(i)$. The variable $s(i)$ generally varies between –255 to +255. Let us experimentally study the probability of s. Figure 1.6 presents these probabilities. We note that:

– they have a well-marked maximum for $s = 0$, which expresses that the zero jump is the most probable;

– they are symmetric;

– they have a very fast and regular decrease.

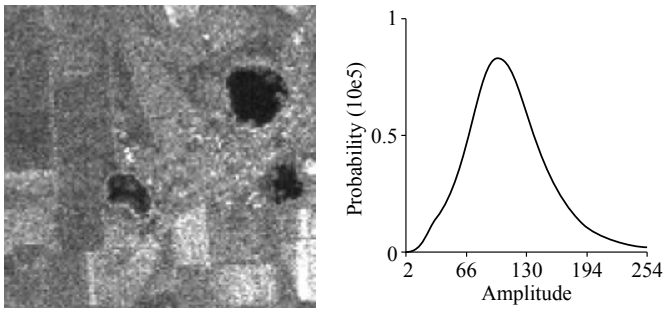

Figure 1.5. *Enlarged lateral radar image (ERS-1 radar) over an agricultural site in Ukraine (© CNES) which shows the importance of the coherent noise and the histogram of the complete scene, which is very close to Rayleigh's law*

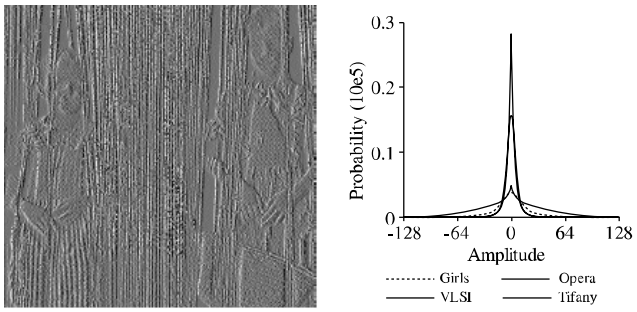

Figure 1.6. *Image of horizontal gradients taken from the "girls" image (value 127 has been added to the overall image) and four jump histograms of four different images*

Seeing these curves, it was proposed to model the probability of a jump in amplitude by a Gaussian of zero average, whose only parameter, the standard deviation σ_s, is a characteristic of the image. The probability of jump s in amplitude can therefore be stated:

$$p(s) = \frac{1}{\sigma_s \sqrt{2\pi}} \exp\left(-\frac{s^2}{2\sigma_s^2}\right) \quad [1.2]$$

Certain images with smooth transitions are characterized by a small value for σ_s, others by a larger value. This field of variation in σ_s is typically between 3 and 15.

It is clear that counter-examples can easily be found in images whose histogram does not have the abovementioned properties. A regular gradation from white to black presents a non-symmetric histogram with uniformly distributed values in the left half-space. A checker board would only present three types of transitions: zero, positive to +255 and negative to –255. These examples do not fit into our hypotheses for normal images.

1.4. The autocorrelation function

1.4.1. *In one dimension*

Another variable, which is of great interest for signal processors, is the autocorrelation function. There are two reasons for this: firstly it expresses in a complete way the spatial dependencies of the signal, secondly it makes it possible to access the Fourier field easily using the Wiener-Kinchine theorem[1].

The autocorrelation function $\gamma_f(k)$ of a discrete function $f(i)$ is defined by:

$$\gamma_f(k) = < f(i) \cdot f^*(i+k) > \quad [1.3]$$

where the symbol $< x >$ expresses the mathematical expectation for the random variable x. The autocorrelation function is usually calculated by:

$$\gamma_f(k) = \sum_{i=-\infty}^{i=+\infty} f(i) \cdot f^*(i+k). \quad [1.4]$$

1 The Wiener-Kinchine theorem establishes that the autocorrelation function is the Fourier transform (FT) from the power spectral density [BLA 81, REF 02].

The images are real signals ($f = f^*$). These are positive signals from which we obtain a mean value $\overline{f}$ to calculate the centered autocorrelation function:

$$\gamma_{f-\overline{f}}(k) = \sum_{i=-\infty}^{i=+\infty} \left(f(i)-\overline{f}\right)\cdot\left(f(i+k)-\overline{f}\right) \qquad [1.5]$$

and we calculate a centered normalized autocorrelation function by bringing this function to its maximum $\gamma_{f-\overline{f}}(0)$ (which is also the variance σ_f^2 of f):

$$C_f(k) = \frac{\gamma_{f-\overline{f}}(k)}{\gamma_{f-\overline{f}}(0)} = \frac{\gamma_{f-\overline{f}}(k)}{\sigma_f^2}, \qquad [1.6]$$

$$C_f(k) = \frac{\Sigma_{i=-\infty}^{i=+\infty}\left(f(i)-\overline{f}\right)\cdot\left(f(i+k)-\overline{f}\right)}{\Sigma_{-\infty}^{+\infty}\left(f(i)-\overline{f}\right)^2}. \qquad [1.7]$$

This function provides numerous interesting properties:

– it has a maximum at the origin (equal to 1);

– it is limited to the interval [–1, +1];

– it is even ($C_f(-k) = C_f(k)$);

– if it has another maximum equal to 1 at another point p, then it has an infinity of maxima at positions np, and is periodic of period p, as well as function f itself;

– there are simple relations between the derivatives of the autocorrelation function and the autocorrelation functions of the derivatives of f.

We present in Figure 1.7 the autocorrelation function of an image for shifts from 1 to 27 points. There is a maximum marked at the origin (often accompanied by a discontinuity of the derivative), followed by a rapid and regular decrease. If we observe the decrease of C_f on a longer field, we note that its amplitudes become very small, expressing a weak correlation of the image pixels very distant from each other.

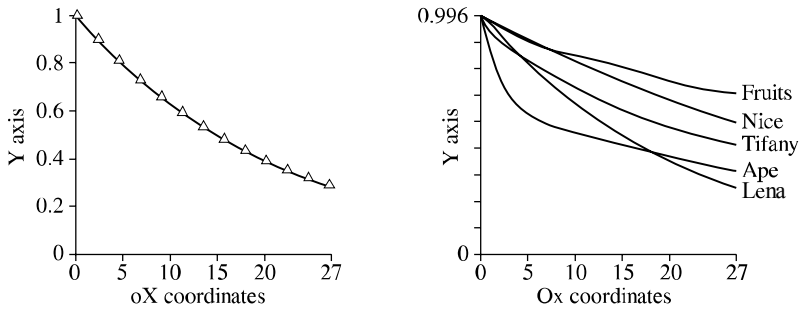

Figure 1.7. *On the left, the measured values of an autocorrelation function (on the "Lena" image) are superimposed on the closest theoretical exponential law, on the right, five correlation functions of different images*

This very general behavior has made it possible to model the normalized centered autocorrelation function by an exponential function:

$$C_f(k) = \exp(-\alpha|k|). \qquad [1.8]$$

Parameter α is the second characteristic parameter of the image, we see in Figure 1.7 that the images with slow variation have a very spread out correlation (and therefore a small α). On the other hand, images with very rapid variations have a pointed autocorrelation and a large α. The field of variation for α is typically from 0.01 to 0.3.

Figure 1.8. *Five images used to calculate the correlations in Figure 1.7: Nice, Fruit, Tiffany, Lena and Ape*

The counter-examples of functions whose autocorrelation is not exponential are easy to find, in particular amongst the periodic functions. If the purely periodic functions are rare in natural images, the images presenting a motif that is repeated over and over (grids, walls, vineyards, fabrics, etc.) abound. Others have average motifs (crowd in the stands, building facades in the street, etc). These images will have an autocorrelation composed of two multiplied motifs: one periodic, the other exponentially decreasing expressing the loss of the motif with distance (see Figure 1.9).

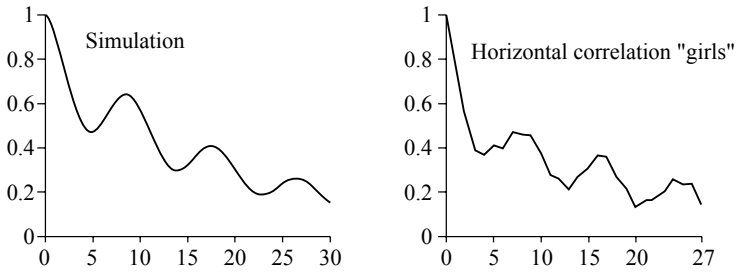

Figure 1.9. *View of the autocorrelation of an image with a strong periodical content: theoretical on the left and measured (on "girls") on the right*

1.4.2. *In multiple dimensions*

If we now consider either the signal not along a line of the image, but according to an unspecified direction, we find a behavior similar to the autocorrelation function with possibly different coefficients α according to the directions. Thus, it would not be surprising to find a strong vertical correlation in a landscape of fir trees while it would be horizontally small. We see in Figure 1.10 the measurements on a real image reflecting this variety. The two-dimensional autocorrelation function $C_f(x,y)$ correctly expresses the isotropic properties of the scene.

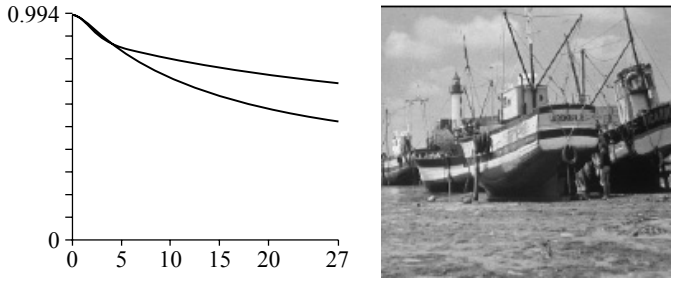

Figure 1.10. *Correlation obtained in the horizontal (top) and vertical (bottom) directions for the "boat" image*

If we want to model this behavior, we are led to choose one of the following two-dimensional models:

$$C_f(x,y) = \exp\left(-\sqrt{(Q(x,y)}\right), \quad [1.9]$$

where $Q(x,y)$ is a quadratic equation in x and y:

$$C_f(x,y) = \exp\left(-\alpha|x| - \beta|y|\right). \quad [1.10]$$

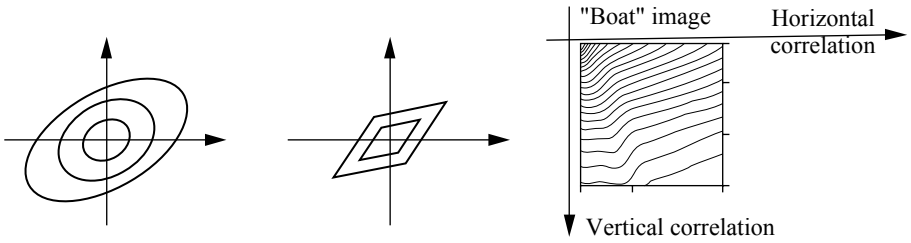

Figure 1.11. *Isocorrelation curves for the non-separable model (on the left) and for the separable model (in the middle) and isocorrelation curves measured on the "boat" image (the lower quarter plane is represented)*

This second form is less satisfying for the continuity of the autocorrelation function, but it is, however, often retained because its separable form makes it easy to use (separation into two independent processes in row and in column), particularly in the Fourier plan (see Figure 1.11).

1.4.3. *The power spectral density*

Arising from the Wiener-Kinchine theorem, the power spectral density will thus have a determined form [BRA 78]. Let F be the FT of f, u the variable associated with the variable of space (spatial frequency), and let us note by P_f the power spectral density of f:

$$P_f(u) = <\left|F(u)\right|^2>, \quad [1.11]$$

$$P_f(u) = \frac{2\alpha}{\alpha^2 + u^2}. \quad [1.12]$$

We see in this function (Lorentz distribution; see Figure 1.12) properties that are well-known by opticians: the energy is at its maximum at the origin (u = 0), i.e., in diffraction theory [FRA 70], on the optic axis, it decreases regularly towards the high spatial frequencies (positive or negative), all the more quickly as the correlation increases (low α).

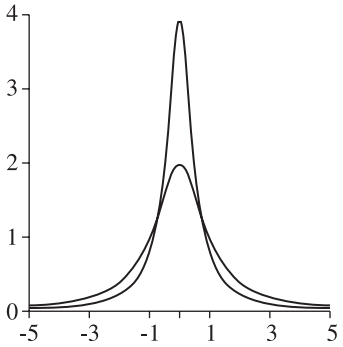

Figure 1.12. *Power spectral density of images with exponential autocorrelation (α = 0.5 and α =1)*

1.5. Entropy

Following Shannon's ideas, entropy is a statistical measurement of the information content of a message. It is therefore adapted to characterizing images, each of which is taken as a specific message.

The idea of entropy[2] relies, of course, on the analogy of physics (Clausius' thermodynamics or Boltzman statistics) and attributes a larger content of information to particularly improbable configurations than to very frequent configurations.

2 This is one of the possible approaches of the definition of the information. Another approach relies on the theory of complexity [DEL 94] and measures the information carried by a message from the length of the smallest program capable of describing this information. This is Kolmogorov's approach [KOL 65]; it is completed by Benett's notion of logical depth which distinguishes complex but calculable sequences from the complex but random sequences using a number of basic steps accomplished by the program to find the information. The curious reader will find in [MAI 96] an application of these image principles.

1.5.1. *Entropy of order 0*

Following the preceding idea, Hartley attributed in 1925 to symbol i emitted by a stationary source with a probability p_i, the quantity of information:

$$I_i = -\log p_i, \qquad [1.13]$$

expressed symbolically in bits if the logarithm is at base 2. Shannon [SHA48] then symbolically defines the mean information or entropy by:

$$S = -\sum_{i=1}^{i=n} p_i \log p_i. \qquad [1.14]$$

Considering an image as a stationary source of pixels, the entropy is thus measured from the only amplitude histogram.

Using the properties of the log$x$ function, we show that the entropy is at its maximum for a uniform spread of probability S_{max} = log n. For the images, this leads most often to an entropy S of less than 8 bits [FAL 66]. The normally encountered numbers are from 4 to 7.5 bits for normally contrasted images, using the essential part of the dynamic of the gray levels.

The effect of a uniform quantification of the image (reduction of gray levels) leads to a regular reduction of the entropy with a slope almost equal to –1 (see Figure 1.13).

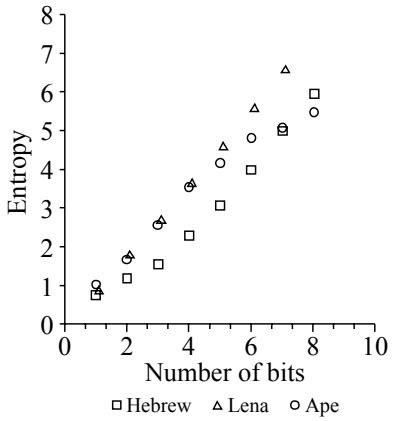

Figure 1.13. *Entropy decrease for three images according to the quantification of gray levels*

We have considered the independent pixels in the preceding lines. Without much more complexity, we can expand the entropy to sources of order N, i.e. for which N successive pixels would be dependent. We would then replace the probability p_i with the joint probability $p_{i,\, i-1,\, \ldots,\, i-N+1}$ of these N pixels.

1.5.2. *Entropy of jumps*

Using the properties underlined above, we can in particular calculate the entropy of jumps in intensity s whose probability is Gaussian:

$$S_s(x) = \frac{1}{2}\log(2\pi e\sigma_s).$$

This entropy has the downside of being negative for very low values of σ_s, but we must take into account the discrete aspect of the quantification levels of the image and replace the obtained continuous result above with its discrete form.

1.5.3. *Conditional entropy, redundancy*

If we consider two exactly superimposable images (for example, two channels of a satellite image or the red channel and green channel of a video signal) that we denote as x_i and y_i the values in a single pixel i, we can definitely define entropy S_x and entropy S_y of each image:

$$S_x = -\sum_{i=1}^{i=n} p(x_i)\log p(x_i),$$

$$S_y = -\sum_{i=1}^{i=n} p(y_i)\log p(y_i),$$

we can equally define the joint entropy of x and y:

$$S_{x,y} = -\sum_{i=1}^{i=n} p(x_i, y_i)\log p(x_i, y_i) \qquad [1.15]$$

but we can also define the conditional entropy of y in relation to x as the mean information, for all values of y, of the conditional information brought about by y knowing x:

$$I_{y|x} = -\log p\left(y|x\right),$$

by averaging over all (x,y) pairs:

$$S_{y|x} = -\sum_{i=1}^{i=n} p\left(x_i, y_i\right) \log p\left(y_i \left| x_i\right.\right).$$

The information brought by x on y is then expressed by:

$$S_{x:y} = S_y - S_{y|x}. \qquad [1.16]$$

We verify that $S_{x:y} = S_{y:x}$.

This size is called the redundancy of x and y. We can verify the following properties:

$$S_{x,y} = S_x + S_{y|x},$$
$$S_{y|x} \leq S_y,$$
$$S_{x:y} = S_x + S_y - S_{x,y}.$$

The predictive coding in use in the 1980s (DPCM coding: differential pulse-code modulation [GUI 96, BAR 02]) relied greatly on research of the best configurations of N pixels making it possible to minimize the conditional entropy of $\left(N+1\right)^e : S_{x_{N+1}|x_1,x_2,..,x_N}$.

1.5.4. *Return on a paradox*

Taking again the small histogram modification exercise presented in section 1.2.2, we can question ourselves on the evolution of the entropy in the course of operations. For example, let us take again the image of the boats whose original entropy was 6.1. After the third histogram modification (see Figure 1.4), its entropy reached 8 bits per pixel. How do we explain this gain in mean information? Where is this information practically located? What can the user do about it?

To answer these questions, we must of course analyze in detail the transformation schemes and, while considering ourselves astute, it is possible to convince ourselves that we can effectively add useful information, for example by giving a less disturbed image (or on the contrary, more contrasted) or by incorporating a parity bit or a different marker making it possible to ensure verifications on transmission integrity, author's identity or other.

1.6. Image models

1.6.1. *Markov-Gauss process*

Starting from the two previously discussed results (probability of Gaussian jumps and autocorrelation to exponential decrease), the idea came rather naturally to propose the following image signal generator model: the image is a Markovian process, in discrete time, and with Gaussian increases.

Let us recall that Markovian processes in discrete time are processes that develop along an ordered succession of instances (here the pixels are along a row) and whose probability to be in state f_i at instant i is dependent only on the state at instant $i-1$: f_{i-1} and of the transition probability $P(f_i|f_{i-1})$ [CUL 75]. If the process is stationary, this probability does not depend on i, but if its increases are Gaussian, so this probability is in the form:

$$P\left(f_i \middle| f_{i-1}\right) = P\left(f_i - f_{i-1}\right)$$
$$= \frac{1}{\sigma_s\sqrt{2\pi}} \exp\left(-\frac{s^2}{2\sigma_s^2}\right), \quad \text{with:} \quad s = f_i - f_{i-1}.$$

The conditional probability $P(f_i|f_{i-1})$ is represented, in the language of Markov chains, by matrix M of size $G \times G$, where G represents the number of gray levels. This results in the following:

$$P\left(f_i\right) = MP\left(f_{i-1}\right).$$

M is a stochastic matrix (sum of columns equals 1 for a given row) but not bi-stochastic. This very simple model is very useful for determining numerous image properties. It has made possible, in particular, numerous works on predictive coding (DPCM) [GUI 96, BAR 02].

This simple model, however, leaves many problems poorly resolved, concerning its two-dimensional extension (we will find such extensions in [GAR 08, HUA 76]

and [HUA 81]), stationarity (difficult to obtain with Markovian processes), but also the causality, adjacent to Markovian processes created for "temporal" processes (voice, queues) [FLE 77]. Causality loses its meaning for images for which there is no irreversible flow of time, unless they were not scanned as for example in television. To recreate a 2D causality imposes arbitraries and we thus define a "past" that can be quarter-plane or half-plane according to need (see Figure 1.14). These reflections are the basis of studies conducted on two-dimensional Kalman filters [WOO 81].

1.6.2. *The mosaic model*

Taking again the properties of the model presented in section 1.6.1 in light of the preceding notes, we note that the major variations with the laws above appear for high transition jumps (the tails of the curves in Figure 1.6) which Gaussian law considerably underestimates. These points are for significant transitions, i.e. image edges. The model in section 1.6.1 assumes a field uniformly covered by a single texture and not varied objects separated by edges.

Can we therefore construct a more realistic model for an image, taking into account all of these properties?

Firstly, the consideration of the non-causal dependencies between pixels has led to the abandonment of the trail of Markov chains to the profit of Markov fields (see Chapter 6). In Markov fields, a pixel no longer depends simply on the 2 or 3 pixels that have preceded it during the regular image scanning, but on a neighborhood that surrounds it and carries the dependencies in a symmetric way between the points (neighborhood of 4 points, or of 8 points in most cases). The disadvantage of Markovian fields is that we can no longer use direct filtering techniques, but must call on iterative techniques that are generally more costly in machine-time, and more difficult to optimize.

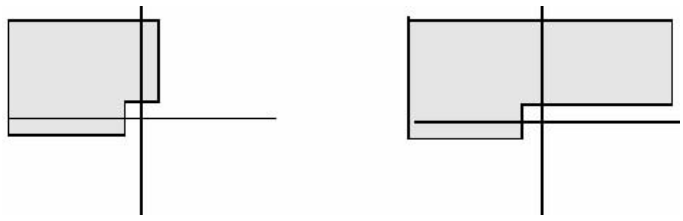

Figure 1.14. *Prediction of a point by "quarter-plane past" (left) and "half-plane past" (right). The gray zones constitute the past of a point at the center of the mark, in the direction of the Markov causality*

The consideration of non-stationarity properties of the images has equally incited authors to abandon the idea of a model that globally expresses the image to the profit of a mosaic model, in which the image consists of a partition of ranges, each revealing a model similar to that developed in section 1.6.1, i.e. each range follows a Markov-Gauss law defined by the mean value $\overline{f}$, the transition probability parameter σ_s and the parameter of correlation decrease α. This model defines two sizes that will be fundamental for image processing: the edges which represent the transitions from one range to another and the textures that describe the statistical properties of each range. This is the model that will be most used for shape recognition, filtering and detection operations. It is also a model that is particularly explored for advanced coding techniques (MPEG-4: object coding [BAR 02]), as well as for the restoration of images while preserving their edges.

1.7. Invariable scaling models

In recent years, another image property has been the object of sustained interest: scaling invariance. We will have the opportunity to address this particular aspect in section 2.4. Statistical scaling invariance expresses the particular behavior of a complex scene for presenting similar structures (edges, textures) to diverse resolutions.

The previously examined laws are not well suited for translating these properties, in particular, as we have already pointed out, the Gaussian laws for jumps underestimate major transitions, important for this process. A study carried out on a large number of images has led to a global model (i.e. adapted to a group statistic over 4,000 images and not on a single image as previously performed) a little different from that in formula [1.2] [HUA 99]. The probability of a jump s is modeled by:

$$p(s) = \frac{1}{Z}\exp\left[-\left|\frac{s}{\tilde{s}}\right|^{\alpha}\right] \qquad [1.17]$$

i.e. a generalized Laplacian distribution. The most adapted parameter α has a value of 0.55, notably less than the Gaussian value of 2. Such a model better expresses the behavior of edges and makes it possible to explain the spectral decrease in the Fourier field. It is, however, less in agreement with the Gaussian model for small jumps as it would predict a more pointed law than that which is practically observed.

These studies are the object of encouraged attention in diverse directions: statistical properties of textures [SRI 02], level line properties or shapes of objects contained in the scene [GOU 00] or statistics in wavelet fields.

1.8. Bibliography

[BAR 02] BARLAUD M., LABIT C., *Compression et codage des images et des vidéos*, Hermes, IC2 Series, Paris, 2002.

[BLA 81] BLANC-LAPIERRE A., PICINBONO B., *Fonctions Aléatoires*, Masson, Sc. et Tech. des Télécoms, Paris, 1981.

[BRA 78] BRACEWELL R.N., *The Fourier Transform and its Applications*, McGraw-Hill, 1978.

[CUL 75] CULLMANN G., *Initiation aux chaînes de Markov, méthodes et applications*, Masson, 1975.

[DEL 94] DELAHAYE J., *Information, complexité et hasard*, Hermes, Paris, 1994.

[EST 69] ESTOURNET D., "Etude statistique d'un signal d'images", *L'Onde Électrique*, p. 510-520, 1969.

[FLE 77] FLEURET J. Holographie et application à divers traitements des images, PhD Thesis, University of South Paris, 1977.

[FRA 70] FRANÇON M., *Vibrations lumineuses – Optique coherente*, Dunod, Paris, 1970.

[GAL 66] GALLAGER R., *Information Theory and Reliable Communication*, John Wiley, New York, 1966.

[GAR 08] GARELLO R. (ed.), *Two-Dimensional Signal Analysis*, ISTE Ltd, London, 2008.

[GOO 76] GOODMAN J., "Some fundamental properties of speckle", *Journal Optical Society of America*, vol. 66, no. 11, p.1145-1150, 1976.

[GOU 00] GOUSSEAU Y., Distribution de formes dans les images naturelles, Thesis, University of Paris IX-Dauphine, January 2000.

[GUI 96] GUILLOIS J.P., *Technique de compression des images*, Hermes, Paris, 1996.

[HUA 76] HUANG T.S., "Picture processing and digital filtering", *Topics in Applied Physics*, vol. 6, 1976.

[HUA 81] HUANG T.S., "Two-dimensional signal processing I", *Topics in Applied Physics*, vol. 42, 1981.

[HUA 99] HUANG J., MUMFORD D., "Statistics of natural images and models", *IEEE Conf. on Comp. Vision and Pattern Recognition*, p. 541-547, 1999.

[KOL 65] KOLMOGOROV A., "Three approaches of the qualitative definition of information", *Information Transmission*, vol. 1, no. 1, p. 9-11, 1965.

[MAI 96] MAÎTRE H., "Entropy, information and image", Maître H., Zinn-Justin J. (eds.), *Progress in Picture Processing*, vol. LVIII, p. 81-117, North Holland, Amsterdam, 1996.

[REF 02] RÉFRÉGIER P., *Théorie du bruit et application en physique*, Hermes, Paris, 2002.

[SHA 48] SHANNON C., "The mathematical theory of communications", *Bell System Technical J.*, vol. 27, p. 379-423, 1948.